ACS OMEGA

http://pubs.acs.org/journal/acsodf

Article

Stable Fatty Acid Solvates of Dasatinib, a Tyrosine Kinase Inhibitor: Prediction, Process, and Physicochemical Properties

Venkata Narasayya Saladi, Bal Raju Kammari, Arthanareeswari Maruthapillai,* Sudarshan Mahapatra, Ramanaiah Chennuru, Eswaraiah Sajja, Srinivasan Thirumalai Rajan, and Vijayavitthal T. Mathad*

Cite This: *ACS Omega* 2022, 7, 7032−7044

Read Online

ACCESS | Metrics & More | Article Recommendations | Supporting Information

ABSTRACT: Exploration of alternate solid forms for dasatinib, a potent oncogene tyrosine kinase inhibitor classified under Biopharmaceutics Classification System (BCS) class II drugs with low water solubility and high permeability, has been performed using COSMO-RS excess enthalpy (Hex) to increase dissolution. The theoretical prediction resulted in the potential for the formation of C_6−C_8 fatty acid solvates with dasatinib. A crystallization process has been identified for the preparation of the predicted solvates and successfully scaled up till the 100 g level. The fatty acid solvates are completely characterized using powder X-ray diffraction (PXRD), differential scanning calorimetry (DSC), thermogravimetric analysis (TGA), Fourier transform infrared (FT-IR) spectroscopy, and proton nuclear magnetic resonance (^{1}H NMR) spectroscopy. Unique powder X-ray diffraction patterns and powder indexing of C_6−C_8 fatty acid solvates indicate the purity of the solid phase. The red shift in the acid carbonyl stretching frequency of C_6−C_8 fatty acids in FT-IR spectra and the intactness of the fatty acid proton in ^{1}H-NMR spectra provide evidence for solvate formation. The stoichiometry of active pharmaceutical ingredients (APIs) with solvent in solvates is measured using TGA and ^{1}H-NMR spectroscopy. Dasatinib C_6−C_8 fatty acid solvates were found to retain their solid form under various stress and pharmaceutical processing conditions. In addition, they exhibited improved powder dissolution over dasatinib Form H1-7 by 2.2-fold. They also showed stability at 40 °C and 75% RH for 3 months. C_8 fatty acid is a USFDA GRAS listed solvent, and hence may be a viable option for drug product development.

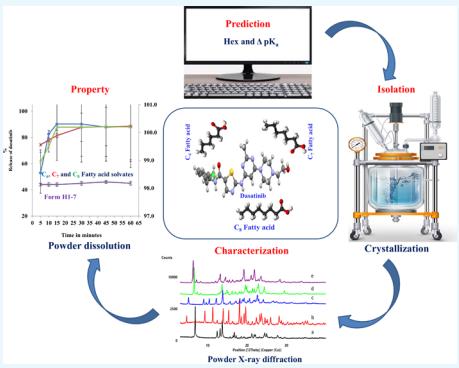

1. INTRODUCTION

The poor aqueous solubility of active pharmaceutical ingredients (APIs) has always been a major challenge in oral drug delivery due to poor absorption, bioavailability, and variation in pharmacokinetics. Approximately 40% of the approved drugs and 90% of the drugs in the discovery pipeline are poorly soluble in water.[1,2] Drug substances are classified under Biopharmaceutics Classification System (BCS) classes I to IV based on their solubility and permeability.[3,4] Pharmaceutical molecules belonging to BCS Classes I and III are ideal over those of classes II and IV in terms of their better biopharmaceutical properties.[5]

Several methods such as molecular modification[6,7] (acceptable salts with ionizable molecules), change in solid-state forms[8] (crystalline to amorphous, metastable polymorphs), co-crystallization,[9] solvate formation with pharmaceutically acceptable solvents,[10] and solid dispersions[11−13] have been reported in the literature for improving apparent solubility and dissolution rate. Among the above approaches, solvate formation (pseudopolymorph) is one of the useful methods to improve physicochemical properties.[14−16] Solvate formation is achieved when drug substances are exposed to different solvents during the crystallization process.[17,18] The crystallization process includes fast solvent evaporation, slow solvent evaporation, recrystallization from the required solvent, vapor diffusion, solvent/antisolvent precipitation, cooling crystallization, and slurry-mediated solvate formation.[19] However, in most cases, solvated forms have challenges toward physical and chemical stability, or in some cases, they may improve chemical stability.[17]

Dasatinib (DAS) is a Bcr-Abl tyrosine kinase inhibitor developed by Bristol-Myers Squibb (BMS) and approved for chronic myelogenous leukemia (CML) and Philadelphia chromosome-positive acute lymphoblastic leukemia under the brand name Sprycel. The molecular structure of DAS is shown in Figure 1. Dasatinib is a BCS class II drug with low solubility and high permeability.[20] Chemically, dasatinib is *N*-(2-chloro-6-methylphenyl)-2-[[6-[4-(2-hydroxyethyl)-1-piperazinyl]-2-methyl-4-pyrimidinyl]amino]-5-thiazole carboxamide

Received: November 30, 2021
Accepted: February 4, 2022
Published: February 15, 2022

https://doi.org/10.1021/acsomega.1c06753
ACS Omega 2022, 7, 7032−7044

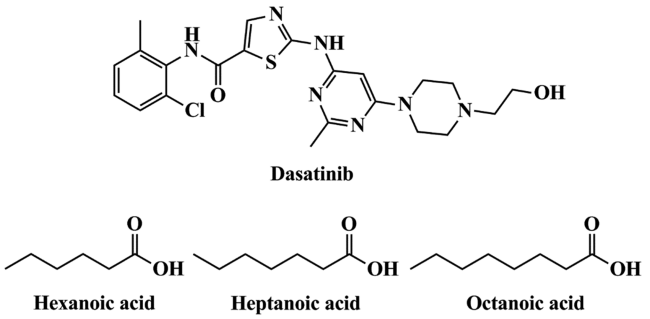

Figure 1. Molecular structures of dasatinib (DAS), hexanoic acid (HA), heptanoic acid (HEA), and octanoic acid (OA).

monohydrate, having two basic nitrogen centers, one in the pyrimidine ring and the other in the piperazine ring, of 5.13 and 7.19 pK_a values, respectively. Further, the molecule also contains one weakly acidic ionization center (−NH group) with a pK_a value of 10.99.[21]

BMS reported several solid forms of dasatinib including monohydrate, butanol, ethanol, and hemiethanol solvates and neat forms such as Form N-6 and Form T1H1-7.[22] The crystal packing efficiency of the dasatinib molecule can be enhanced by incorporating a solvent or water molecule. Due to a higher packing efficiency, dasatinib is a promiscuous solvate former, which is evidenced by the report of more than 60 solvates of dasatinib.[23−27]

Matzger et al.[27] reported the structural aspects of commercialized hydrate forms (BMS, Form H1-7) and anhydrous forms (BMS, Form N-6). They showed solubility advantage of the dasatinib anhydrate form over the hydrate form at ∼23 °C with limitations in the stability of the anhydrate form during the solubility study. Orola et al.[25] reported 26 solvated forms of dasatinib, provided the structural relationship among the studied solvates, and grouped them accordingly. Recently, Rohani et al.[26] reported a new crystal structure of dasatinib methanolate and studied the transient nature of the methanolate and variation in anhydrous outcomes by applying different desolvation techniques. Methanolate solvate's transient nature leads to the benefit of particle size reduction. Exploration of higher-chain C_6−C_9 fatty acid solvates to improve the physicochemical properties of drug product development is not well studied in the available pharmaceutical literature. Fatty acid solvates for one of the drug substances Griseofulvin, an antifungal medication, were reported by Abougela and Grant in 1979,[28] and recently, Ibrutinib fatty acid solvates have been reported.[29] There is no detailed report on alternate solvate forms of dasatinib with respect to their pharmaceutical processability, stability, and physicochemical aspects. This motivated us to explore fatty acid solvates/alternate solvates of dasatinib to study the abovementioned pharmaceutical aspects.

In the present study, we have explored alternate solid forms of dasatinib based on the prediction using COSMO-RS software and the ΔpK_a rule. The potential for the formation of hexanoic acid (HA), heptanoic acid (HEA), and octanoic acid (OA) solvates with dasatinib (DAS) has been obtained according to the prediction outcome. The predicted dasatinib hexanoic acid (DAS-HA) solvate, dasatinib heptanoic acid (DAS-HEA) solvate, and dasatinib octanoic acid (DAS-OA) solvate are novel solvates of DAS and are prepared using the crystallization method and scaled up till the 100 g level. The obtained DAS-HA, DAS-HEA, and DAS-OA were characterized using different crystallographic, spectroscopic, and thermal techniques. All of the novel solid forms such as DAS-HA, DAS-HEA, and DAS-OA were studied for accelerated stress stability at 40 °C and 75% RH, high-temperature stress, high humidity, pharmaceutical process stress, and powder dissolution as per International Conference on Harmonization (ICH),[30] and the results are presented in this report.

2. RESULTS AND DISCUSSION

2.1. Prediction of DAS-HA, DAS-HEA, and DAS-OA Formation Using COSMOthermX and the ΔpK_a Rule. COSMO-RS software can predict solvate or co-crystal formation behavior by calculating the excess enthalpy (Hex)[31−34] of the subjected molecules of interest. The negative high numeric enthalpies (Hex) of a solvent and an API indicates a higher probability of solvate formation. Hence, we have used this tool to shortlist the probable solvents that may be prone to forming solvates with dasatinib. The list of probable solvents with their corresponding Hex values is shown in Table 1. The predicted excess enthalpy values favor solvate formation of DAS with HA, HEA, and OA.

Table 1. Excess Enthalpy Calculation of DAS with Various Solvents

s. no.	solvent	Hex
1	hexanoic acid	−1.34
2	heptanoic acid	−1.07
3	octanoic acid	−0.19
4	water	−0.12
5	ethanol	0.116
6	2-butanol	0.161
7	1-butanol	0.162

The possibility of salt or co-crystal formation between participating molecular components (acid and base) can be predicted using the ΔpK_a rule.[35] This rule predicts the possibility of proton transfer from the participating acid to the base molecular component. In general, if the pK_a difference between conjugate acid (base) and acid is less than 3.0, co-crystal formation can be expected, and if it is more than 3.0, salt formation is expected.[36] In the co-crystal, the co-former exists as a solid at ambient conditions before forming co-crystals, whereas the co-former is in the liquid state at ambient conditions before forming a solvate.[37] Hence, the ΔpK_a rule can be applied to predict the solvate formation over salt formation. In the current study, pK_a values of DAS, HA, HEA, and OA were calculated using online free software ChemAxon PASS. The pK_a and ΔpK_a values of DAS and HA, HEA, and OA are shown in Table 2. The calculated ΔpK_a values between dasatinib and HA, HEA, and OA solvents are less than 3.0. The predicted excess enthalpy values and Δ pK_a (<3) values favor the solvate formation between DAS and HA, HEA, and OA. In addition, theoretically predicted DAS-HA, DAS-HEA, and DAS-OA were experimentally isolated using the crystallization method in the batch size of 100 g (equivalent to dasatinib) with remarkable yield.

2.2. Powder X-ray Diffraction. Powder X-ray diffraction (PXRD) is a prime characterization tool for probing the identity and uniqueness of the condensed crystalline solid phase of any material.[38] PXRD patterns of the prepared DAS-HA, DAS-HEA, and DAS-OA exhibited unique Bragg peaks

https://doi.org/10.1021/acsomega.1c06753
ACS Omega 2022, 7, 7032−7044

Table 2. pK_a and ΔpK_a Values of DAS, HA, HEA, and OA

description	pK_a value	ΔpK_a
DAS (piperazine nitrogen)	7.19	2.1
HA (acid)	5.09	
DAS (pyrimidine nitrogen)	5.13	0.04
HA acid (acid)	5.09	
DAS (piperazine nitrogen)	7.19	2.04
HEA acid (acid)	5.15	
DAS (pyrimidine nitrogen)	5.13	−0.02
HEA (acid)	5.15	
DAS (piperazine nitrogen)	7.19	2
OA (acid)	5.19	
DAS (pyrimidine nitrogen)	5.13	−0.06
OA acid (acid)	5.19	

(Figure 2 and Table 3) when compared to Form N-6 and H1-7.

2.3. Powder Indexing. The phase purity of a polycrystalline material can be unambiguously identified by indexing the powder X-ray diffraction pattern.[39] In the current work, Material Studio (version 2019) was used to index and refine the PXRD patterns of DAS-HA, DAS-HEA, and DAS-OA. The selected programs for indexing were X-cell[40]/Dicvol.[41] The space group selection is automatic in this reflux module of Material Studio. The Pawley refinement is a least-square fit to calculate patterns. In this approach, the effectiveness of fit between measured and calculated patterns can be identified by a figure of merit (R_{wp}).[41] The same approach is considered for PXRD pattern refinement of DAS-HA, DAS-HEA, and DAS-OA. The powder indexing results are provided in Table 4, and Pawley profile fit PXRD patterns of DAS-HA, DAS-HEA, and DAS-OA are shown in Figures 3−5, respectively. The results indicate that DAS-HA, DAS-HEA, and DAS-OA are phase-pure and unique.

2.4. Thermal Analysis. DSC and TGA were utilized for identifying the solvate or hydrate formation.[42,43] In addition, significant information about the lattice bound and/or physically sorbed solvent in the solid phase is obtained.

2.4.1. DAS-HA. The DSC thermogram of DAS-HA shows five endothermic event peak values at 121.35, 151.68, 189.53, 225.81, and 279.28 °C (Figure 6a). To understand the multiple DSC transitions, TGA analysis (Figure 6b) was performed. In the TGA analysis, surface solvent/moisture was observed till 70 °C with a weight loss of 0.31%. The corresponding 0.31% weight loss is supported by the water content analysis by Karl Fischerln (KF) titration and *n*-heptane solvent content analysis by gas chromatography (GC) (SI, Table S1). A weight loss of 42.40% from 70 to 150 °C in the TGA thermogram corresponded to the first endotherm observed in DSC at 121.13 °C. This percentage weight loss is theoretically equivalent to 3 mol of HA solvent in DAS-HA and reveals the stoichiometry ratio of 1:3 for DAS and HA.

Table 3. Characteristic Peak Positions of DAS Solid Forms

form	characteristic peak °2θ (±0.2)
DAS Form N-6/anhydrate	6.8, 11.1, 12.3, 13.2, 13.7, 16.7, and 24.3
DAS Form H1-7	4.6, 11.2, 18.0, 18.4, 19.2, 19.6, and 24.5
DAS-HA	7.43, 8.40, and 12.79
DAS-HEA	6.4, 8.3, 7.25, 12.13, and 28.36
DAS-OA	5.17, 9.0, 9.64, and 10.40

No significant weight loss (0.23%) was observed from 150 to 250 °C. This temperature range has three endothermic events in DSC (151.68, 189.53, and 225.81 °C). To understand these three DSC transitions, a temperature-cycled PXRD study was performed. The temperature-cycled PXRD pattern was similar to that of Form N-6 with a few unknown peaks as shown in Figure 7a,b. The unknown peaks (arrows marked) were found to be related to the 225.81 °C endotherm in DSC. The DSC and TGA overlay thermograms of temperature-cycled DAS-HA are shown in SI, Figures S1 and S2.

This indicates that the solid−solid transition or the mixture of polymorphs generated during the desolvation of DAS-HA may have melting points at 151.68, 189.53, and 225.81 °C. The final DSC endotherm of DAS-HA at 279.28 °C corresponded to the melting of DAS Form N-6.

2.4.2. DAS-HEA. The DSC thermogram of DAS-HEA shows four endothermic event peak values at 100.80, 175.14, 246.70, and 279.10 °C (Figure 8a). To interpret the multiple DSC events, TGA analysis was performed. The TGA thermogram shows four weight-loss events (Figure 8b). The first weight loss of 0.49% till 70 °C is attributed to the loss of surface water, *n*-heptane, and HEA (SI, Table S1). The second weight loss of 36.6% from 70 to 128 °C and the third weight loss of 7.61% from 128 to 180 °C in TGA (total weight loss of 44.26%) correspond to the portionwise loss of 3 mol of HEA from DAS-HEA, indicating a stoichiometric ratio of 1:3 for DAS and HEA. This has been further confirmed by the ^{1}H NMR study (SI, Figure S20).

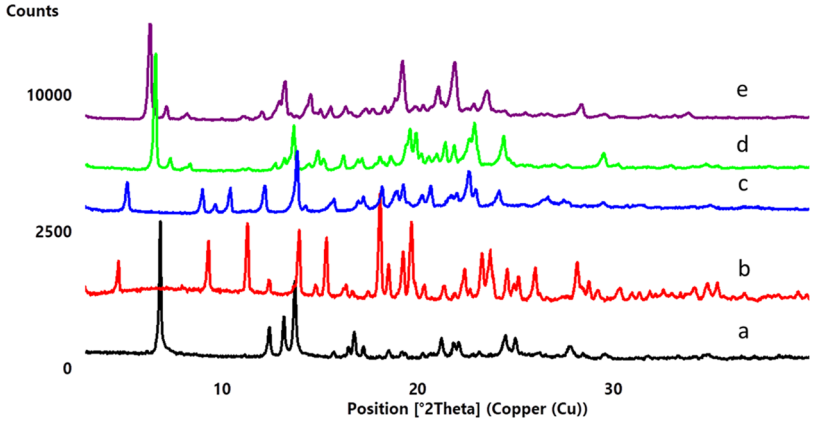

Figure 2. Overlaid PXRD patterns of (a) DAS Form N-6, (b) DAS Form H1-7, (c) DAS-OA, (d) DAS-HA, and (e) DAS-HEA.

https://doi.org/10.1021/acsomega.1c06753
ACS Omega 2022, 7, 7032−7044

Table 4. Crystallographic Information on DAS-HA, DAS-HEA, and DAS-OA

crystal data	DAS-HA	DAS-HEA	DAS-OA
chemical formula	$(C_{22}H_{26}ClN_7O_2S)_1 \cdot (C_6H_{12}O_2)_3$	$(C_{22}H_{26}ClN_7O_2S)_1 \cdot (C_7H_{14}O_2)_3$	$(C_{22}H_{26}ClN_7O_2S)_1 \cdot (C_8H_{16}O_2)_1$
M_r	836.49	878.571	632.224
T K	298	298	298
crystal system	monoclinic	monoclinic	triclinic
space group	$P2_1$	$P2_1$	$P\text{-}1$
a Å	17.9133	27.42095	14.32210
b Å	13.0923	13.38177	12.49535
c Å	15.3045	12.24202	8.55480
α°	90	90	93.13639
β°	113.5955	104.80127	99.09879
γ°	90	90	104.82027
V Å^3	3635.10	4343.07	1454.15
Z	2	4	2
final R_p	6.26%	5.87%	6.83%
final R_{wp}	9.47%	9.35%	9.66%
final R_{wp} (without background)	17.81%	12.95%	15.78%
diffraction data	powder	powder	powder
radiation	Cu Kα λ =1.5406 Å	Cu Kα λ =1.5406 Å	Cu Kα λ =1.5406 Å
instrument	Bruker	Bruker	Bruker

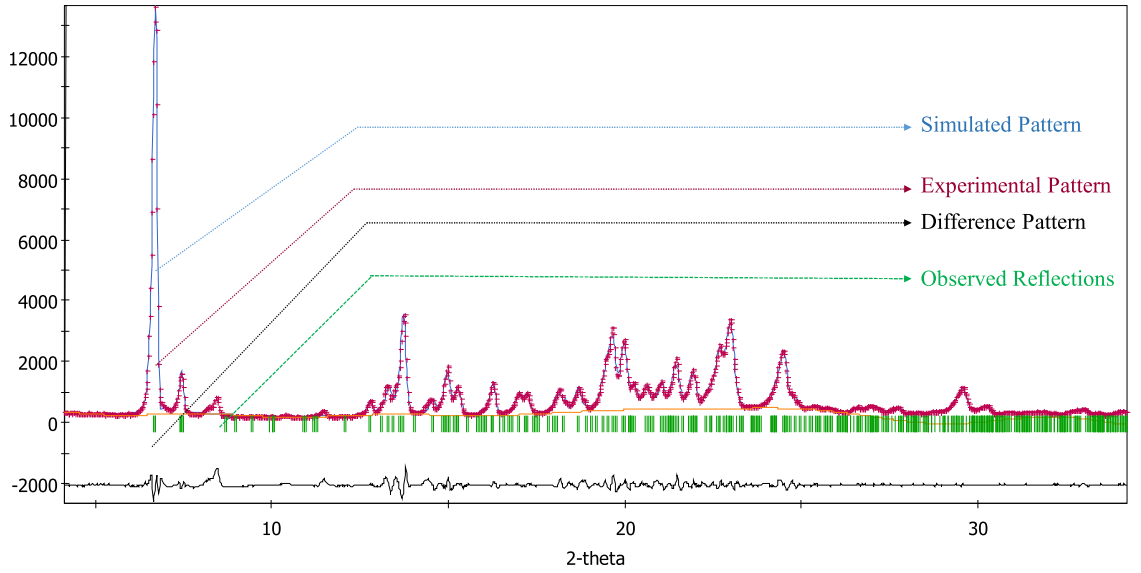

Figure 3. Pawley profile fit PXRD patterns of DAS-HA.

The first endothermic event (100.81 °C) in the DSC thermogram and the second broad endotherm at 180 °C are attributed to the desolvation of HEA. Further, no significant weight loss (0.2%) was observed in TGA from 180 to 250 °C. To understand the third endothermic event in DSC at 246.70 °C, DAS-HEA was subjected to temperature-cycled PXRD analysis. The PXRD pattern is found to be that of Form N-6 with a few unknown peaks (Figure 9a,b). The PXRD peaks of the unknown phase are highlighted in Figure 9b with arrow marks. The DSC and TGA overlay thermograms of temperature-cycled DAS-HA are shown in the SI, Figures S3 and S4.

Hence, we presume that the 246.70 °C event in DSC may be due to solid−solid transition or melting of an unknown form that is generated during the HEA desolvation. The fourth endothermic event (279.10 °C) in DSC is related to the melting of dasatinib Form N-6.

2.4.3. DAS-OA. DSC and TGA overlay thermograms of DAS-OA are shown in Figure 10a,b. The first endothermic event (peak value) in DSC at 152.75 °C is related to the desolvation of OA. This event is complemented by a TGA weight loss of 22.27% (Figure 10b) between 100 and 155 °C, which is equal to a 1:1 stoichiometric ratio of DAS and OA. The second endothermic event in DSC is a heat capacity baseline step-up event from 167 to 172 °C. This step-up event in DSC could be due to a molecular rearrangement of desolvated DAS-OA to DAS Form N-6. To understand this, a temperature-cycled PXRD analysis is performed. The post-temperature-cycled PXRD pattern shows the conversion of DAS-OA to Form N-6 (Figure 11b), which has a corresponding DSC melting peak at 284.19 °C. The DSC and TGA overlay thermograms of temperature-cycled DAS-HA are shown in the SI, Figures S5 and S6. A minor weight-loss event of 0.36% from 155 to 172 °C in TGA corresponds to the loss of residual octanoic acid solvent after a major lattice solvate loss.

https://doi.org/10.1021/acsomega.1c06753
ACS Omega 2022, 7, 7032−7044

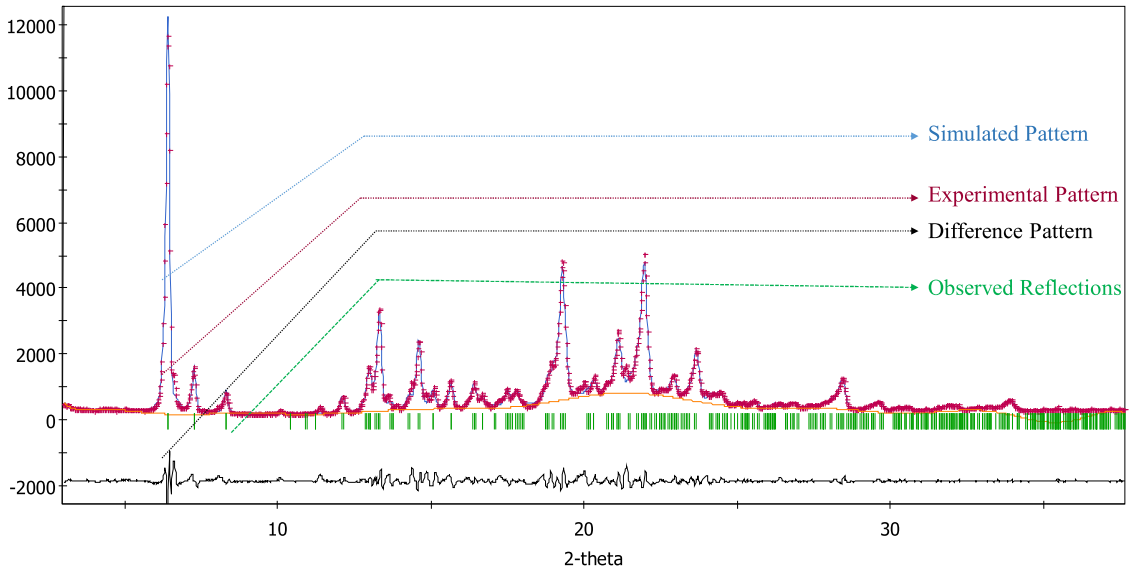

Figure 4. Pawley profile fit PXRD patterns of DAS-HEA.

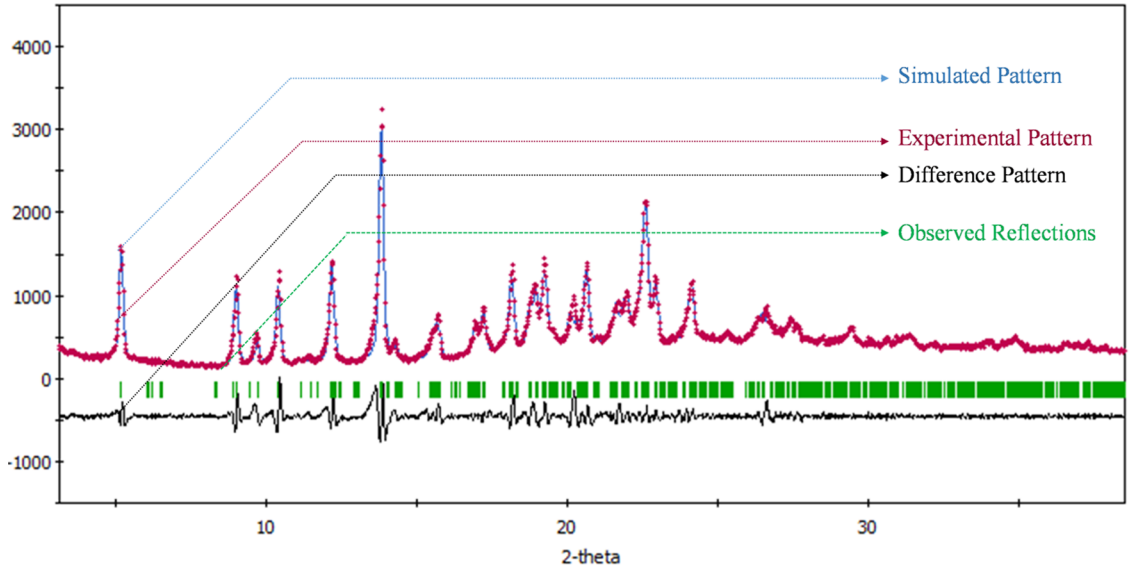

Figure 5. Pawley profile fit PXRD patterns of DAS-OA.

2.5. FT-IR Spectroscopy. Salt and solvate formation between a carboxylic acid and a base can be easily identified using FT-IR spectroscopy.[44] In the case of salt formation between a carboxylic acid and a base, the acid carbonyl stretching frequency should disappear from the spectra and two new stretching frequencies of carboxylate anion (symmetric and asymmetric) should appear at lower FT-IR wavenumbers (lowered by ∼100 cm^{-1}). To understand the salt or solvate formation between HA, HEA, and OA with DAS, a detailed FT-IR study is performed, and results are presented herewith. Neat HA, HEA, and OA solvents showed −C═O stretching frequencies at 1709.43, 1710.53, and 1713.34 cm^{-1}, respectively (SI, Figures S7−S9). The newly prepared DAS-HA, DAS-HEA, and DAS-OA show fatty acid carbonyl stretching frequencies at 1696.90, 1692.03, and 1651.34 cm^{-1}, respectively (SI, Figures S11−S13). The appearance of lower carbonyl stretching frequencies than individual fatty acid carbonyl stretching frequencies is evidence of solvate formation (SI, Figure S14). Further, DAS Form N-6 showed an amide carbonyl vibrational stretching frequency at 1619.70 cm^{-1} (Table 5 and SI, Figure S10). The amide carbonyl stretching frequencies of DAS-HA and DAS-HEA were observed at 1629.35 and 1630.45 cm^{-1}, respectively, and in the case of DAS-OA, it was observed at 1613.62 cm^{-1} (Table 5 and SI, Figures S11−S13). This also indicates the presence of hydrogen bonds between DAS and fatty acid solvent molecules in the crystal lattice of DAS-HA, DAS-HEA, and DAS-OA.

2.6. ^{1}H Nuclear Magnetic Resonance Spectroscopy. Solution ^{1}H NMR spectroscopy is a very widely useful technique for determining the stoichiometry of salt, solvate, and co-crystal formers.[45,46] In the current study, proton NMR spectroscopy was used to probe the stoichiometry between HA, HEA, and OA fatty acids with DAS. It was also used to identify whether the newly prepared DAS-HA, DAS-HEA, and DAS-OA exist as salt or solvate. The absence or presence of the −COOH proton of HA, HEA, and OA was examined in the ^{1}H NMR spectra of DAS-HA, DAS-HEA, and DAS-OA to

https://doi.org/10.1021/acsomega.1c06753
ACS Omega 2022, 7, 7032−7044

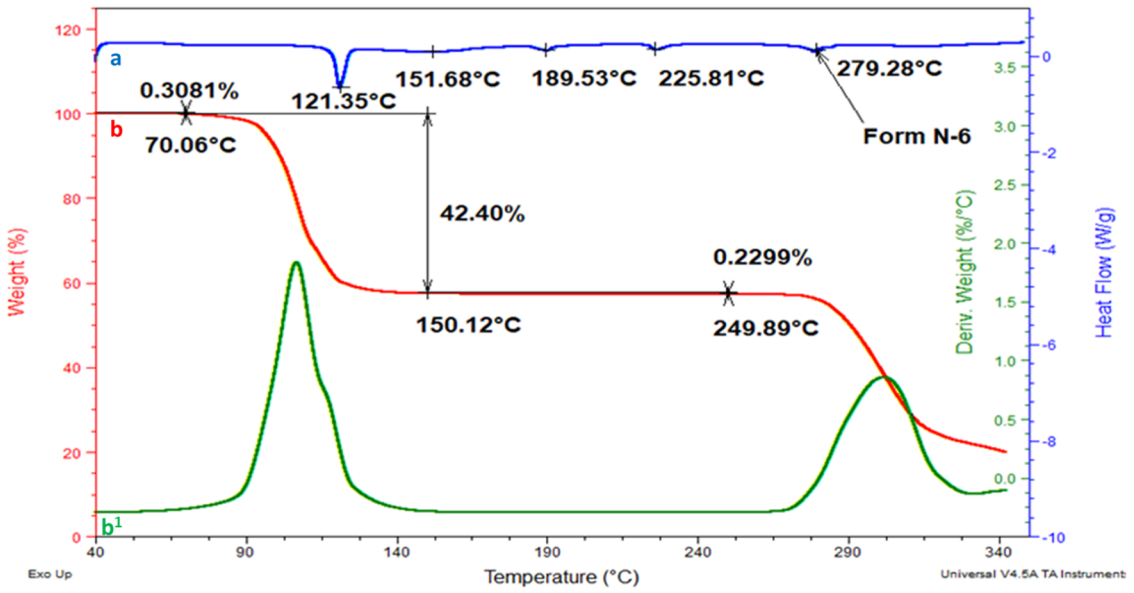

Figure 6. DAS-HA overlay thermograms for (a) DSC, (b) TGA, and (b^1)TGA derivative.

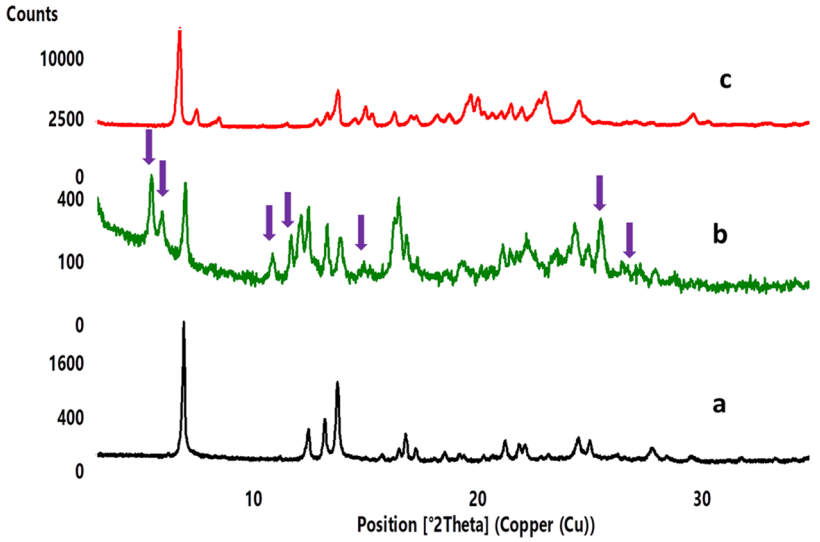

Figure 7. PXRD overlay patterns of (a) DAS Form N-6, (b) temperature-cycled DAS-HA, and (c) input DAS-HA.

identify the salt or solvate formation. The proton NMR spectra of neat fatty acids (HA, HEA, and OA) showed terminal methyl protons with a peak area of ∼3.0 between 0.839 and 0.874 δ_{ppm} (Table 6 and SI, Figures S15−S17). The neat DAS also has two methyl groups in its molecular structure, one on the chlorobenzene ring and the other on the pyrimidine ring. These methyl groups do not interfere with the methyl proton signals of HA, HEA, and OA (SI, Figure S18), and hence, HA, HEA, and OA methyl protons are selected for understanding the stoichiometry (mole ratio) of solvent and DAS. The presence of protons pertaining to −COOH in ^{1}H NMR spectra of DAS-HA, DAS-HEA, and DAS-OA with slightly deshielding (δ_{ppm}), indicating solvate formation (SI, Figures S19−S21). The ^{1}H NMR data of DAS-HA, DAS-HEA, and DAS-OA are shown in Table 6. Based on the proton area integration, it is understood that DAS-HA and DAS-HEA exist in a 1:3 mole ratio whereas DAS-OA shows a 1:1 mole ratio (SI, Figure S21). The ^{1}H NMR results comply with the TGA weight-loss percentage with respect to stoichiometry and FT-IR results with respect to solvate formation. Finally, TGA, FT-IR, and ^{1}H NMR results support solvate formation between dasatinib and fatty acid solvents.

2.7. Confirmation of Solvates (DAS-HA, DAS-HEA, and DAS-OA) Using Hot Stage Microscopy (HSM), ^{1}H NMR, and Temperature-Cycled PXRD Studies. To obtain structural insights into the DAS-HA, DAS-HEA, and DAS-OA solvates, we extensively tried to grow the single crystals using various crystallization techniques, but our trials were unsuccessful in obtaining mountable single crystals; hence, we used orthogonal techniques to confirm solvate formation. To provide structural confirmation of the solvates unambiguously, we used several orthogonal techniques such as HSM,[47] ^{1}H NMR, and temperature-cycled PXRD studies. All DAS fatty acid solvates show the final endothermic event in the DSC thermogram from 279.10 to 284.19 °C (Figures 6a, 8a, and 10a).

To understand the actual event of peaks in DSC, we performed a HSM analysis. The HSM study revealed that the

https://doi.org/10.1021/acsomega.1c06753
ACS Omega 2022, 7, 7032−7044

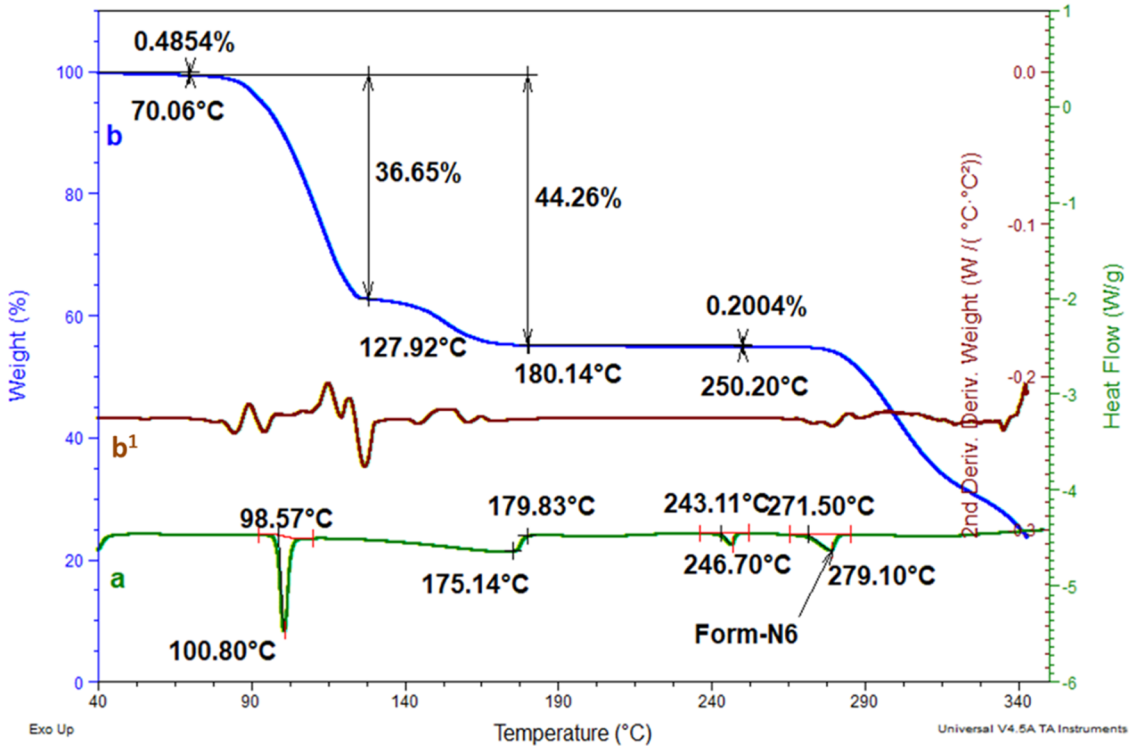

Figure 8. DAS-HEA overlay thermograms for (a) DSC, (b) TGA, and (b^1) TGA derivative.

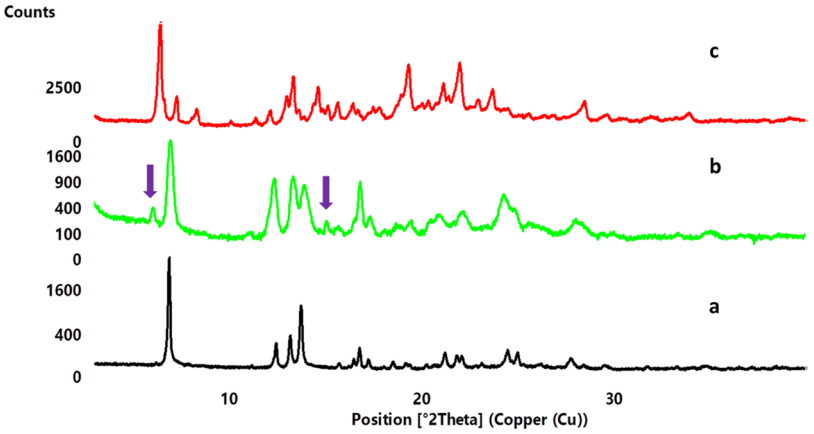

Figure 9. PXRD overlay patterns of (a) DAS Form N-6, (b) temperature-cycled DAS-HEA, and (c) input DAS-HEA.

endothermic event (peak value) observed in DSC for DAS-HA at 121.35 °C, DAS-HEA at 100.80 °C, and DAS-OA at 152.75 °C was related to desolvation (SI, Figures S22−S24) as there was no change in the primary morphology of needlelike particles of DAS-HA, DAS-HEA, and DAS-OA solvates at 120, 110, and 155 °C, except for slight fading of the appearance of needles. Further, this observation is also in accordance with TGA weight-loss events of solvates (Figures 6b, 8b, and 10b). The melting temperatures of DAS-HA, DAS-HEA, and DAS-OA observed at 279.1, 286.9, and 284.1 °C, respectively, in HSM (SI, Figure S25a−c) are in line with the melting peaks of Form N-6 observed in the DSC thermogram (Figures 6a, 8a, and 10a).

To understand the chemical entity associated with melting events of all DAS solvates (at ∼279.1 to 286.9 °C) in HSM, we individually heated DAS-HA, DAS-HEA, and DAS-OA using a thermogravimetric analyzer until 250 °C with a 10 °C/min ramp, followed by cooling to 30 °C. During the above process, the materials were desolvated. The desolvated solvates were subjected to PXRD analysis. The resultant PXRD patterns of DAS-HA, DAS-HEA, and DAS-OA matched that of the reported dasatinib anhydrate (Form N-6, SI, Figure S26b−e). The crystal structure for the reported dasatinib free base anhydrate (N-6) is already solved in the literature (SI, Figure S27).

Further, the above-desolvated DAS-HA, DAS-HEA, and DAS-OA solids were subjected to ^{1}H NMR analysis, and it was observed that the protons corresponding to HA, HEA, and OA were absent (SI, Figures S28−S30), indicating the dasatinib Form N-6/anhydrate base (SI, Figure 31a−d). This is unambiguous evidence to show that DAS can only form solvates with HA, HEA, and OA fatty acids. If DAS had formed salts with HA, HEA, and OA, the resultant molecular structure of dasatinib would have become a dasatinib cation/conjugate

https://doi.org/10.1021/acsomega.1c06753
ACS Omega 2022, 7, 7032−7044

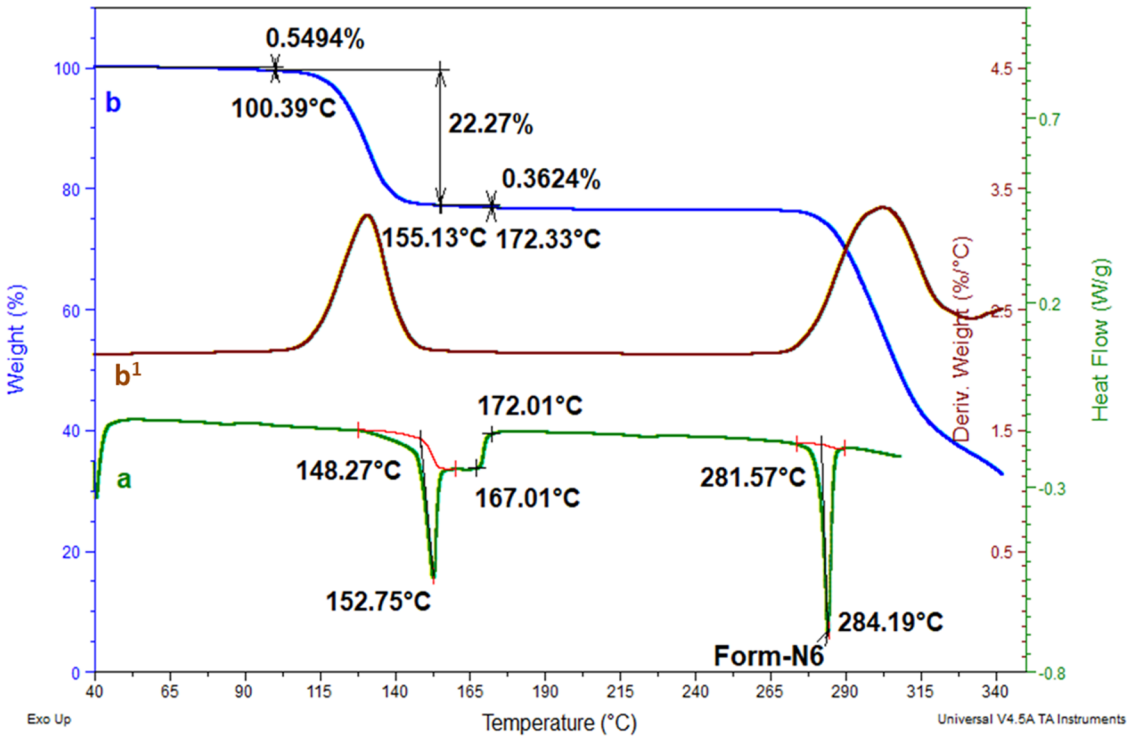

Figure 10. DAS-OA overlay thermograms (a) DSC, (b) TGA, and (b^1) TGA derivative.

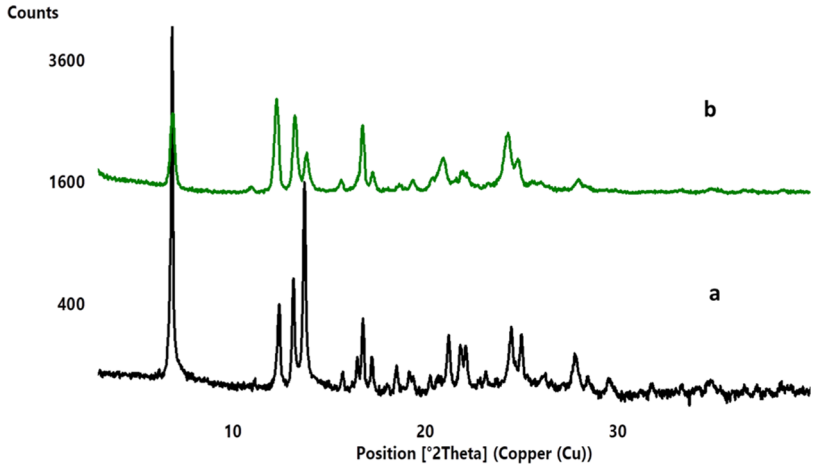

Figure 11. PXRD overlay pattern of (a) DAS Form N-6 and (b) temperature-cycled DAS-OA.

Table 5. FT-IR Stretching Frequencies of DAS, Fatty Acids, and DAS Fatty Acid Solvates

description	acid −C═O stretching frequency (cm^{-1})	amide C═O stretching frequency (cm^{-1})
HA	1709.43	
HEA	1710.53	
OA	1713.34	
DAS Form N-6		1619.70
DAS-HA	1696.90	1629.35
DAS-HEA	1692.03	1630.45
DAS-OA	1651.34	1613.62

Table 6. ^{1}H NMR DAS, Fatty Acids, and DAS Fatty Acid Solvates

description	δ_{ppm} of acid methyl protons	δ_{ppm} of acid proton	proton area (methyl and acid)
DAS			
HA	0.840−0.874	11.954	3 and 0.97
HEA	0.839−0.873	11.951	3 and 0.94
OA	0.839−0.873	11.949	3 and 0.96
DAS-HA	0.839−0.874	11.945	9.54 and 3.14
DAS-HEA	0.836−0.871	11.884	9.21 and 3.84
DAS-OA	0.838−0.873	11.937	3.34 and 0.96

acid with the covalent bonded hydrogen at the piperazine moiety and would have led to decomposition without converting into the known free base anhydrate/Form N-6. Hence, DAS can only form solvates with HA, HEA, and OA fatty acids.

2.8. Physicochemical Properties. *2.8.1. Powder Dissolution.* Powder dissolution study is a well-known pivotal test

https://doi.org/10.1021/acsomega.1c06753
ACS Omega 2022, 7, 7032−7044

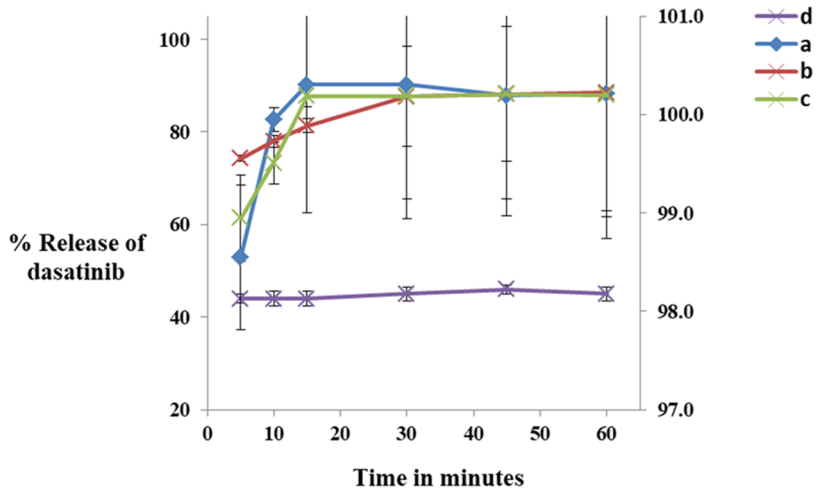

Figure 12. Powder dissolution overlay patterns of (a) DAS-HA, (b) DAS-HEA, (c) DAS-OA, and (d) DAS Form H1-7.

for drug substance performance, and it is very useful in predicting the *in vivo* performance of drug products.[48,49] To determine the comparative dissolution profiles of dasatinib Form H1-7 with DAS-HA, DAS-HEA, and DAS-OA in the maximum daily dosage range (140 mg equiv to dasatinib), the powder dissolution study was conducted in acetate buffer (at pH 4) with 1% Triton-X (USFDA Office of Generic Drug media for dasatinib) medium under sink conditions. DAS-HA, DAS-HEA, and DAS-OA showed ∼100% drug release within 10 min of dissolution time point, whereas Form H1-7 showed 45% of drug release after 60 min (Figure 12 and SI, Table S2). In addition, precipitation of dasatinib is not observed from the dissolution medium in the case of DAS-HA, DAS-HEA, and DAS-OA even after completion of the dissolution study. Thus, DAS-HA, DAS-HEA, and DAS-OA exhibited a superior dissolution rate of 2.2-fold over DAS Form H1-7 (monohydrate).

2.8.2. Process-Induced Transformation. Milling, compaction, and aqueous and nonaqueous granulation are common pharmaceutical process operations during drug product manufacturing.[50,51] A solid form should be robust to bear all of the mentioned processes to make a viable pharmaceutical drug product for oral route delivery. Hence, we tested the tolerance of solid form intactness of isolated DAS-HA, DAS-HEA, and DAS-OA forms under milling, compaction, and aqueous slurry. The solvates showed retention of their solid forms when subjected to pharmaceutical process operations (SI, Table S3 and Figures S32−S34).

2.8.3. Stress, Humidity, and ICH Stability. Many pharmaceutical solvates can pose a challenge with respect to their solid form intactness upon exposure to high humidity, stress, and stability conditions. In the current work, synthesized DAS-HA, DAS-HEA, and DAS-OA were exposed to high humidity (90% RH) and high-temperature stress at 60 °C for 48 h. In addition, we performed stability studies at accelerated conditions (40 °C and 75% RH) for 3 months. The solid form intactness and significantly low water pickup indicate that the solvates are slightly hygroscopic. However, the other stress conditions indicate that the solvates are robust and stable. The results are shown in SI, Table S4 and Figures S32−S34.

3. CONCLUSIONS

We predicted the novel solvates, dasatinib hexanoic acid (DAS-HA), dasatinib heptanoic acid (DAS-HEA), and dasatinib octanoic acid (DAS-OA) for dasatinib, a tyrosine kinase inhibitor, using COSMO-RS excess enthalpy theoretical calculation and the ΔpK_a rule. The predicted solvates were successfully prepared using a crystallization process at a 100 g scale. The novel solvate forms were characterized using PXRD, DSC, TGA, FT-IR, and ^{1}H NMR techniques. Phase purity and uniqueness of the fatty acid solvates were confirmed using the X-ray powder diffraction data indexing method. The stoichiometry of solvates was probed using ^{1}H NMR spectroscopy and TGA. It is found that the mole ratio of DAS-OA is 1:1, whereas for DAS-HA and DAS-HEA, the mole ratio was found to be 1:3. Solvate formation in DAS-HA, DAS-HEA, and DAS-OA is confirmed using HSM, temperature-cycled PXRD, and ^{1}H NMR spectroscopy of desolvated solvates. The isolated fatty acid solvates were slightly hygroscopic and retained their pseudopolymorphic identity in regular pharmaceutical process operations such as milling, compaction, high-temperature stress at 60 °C, and aqueous slurry. DAS-HA, DAS-HEA, and DAS-OA are stable at 40 °C and 75% RH for 3 months and show a 2.2-fold increase in powder dissolution rate over DAS Form H1-7. Further, OA is a USFDA GRAS listed molecule,[52] and hence, DAS-OA may be a viable option for the drug product development of dasatinib.

4. MATERIALS AND METHODS

4.1. Materials. Dasatinib Form N-6 (HPLC purity >99%), hexanoic acid (HA), heptanoic acid (HEA), octanoic acid (OA), and *n*-heptane were gifted by MSN Laboratories Pvt. Limited, Hyderabad. Solvents (purity >99%) and other chemicals were purchased from Finar Chemicals (India). Milli-Q water used in all of the experiments was purified using resin filters and deionized to a high degree using a water purification system manufactured by Millipore Corporation.

4.1.1. Dasatinib Monohydrate. Dasatinib monohydrate (Form H1-7) was prepared as per the procedure mentioned in the Bristol-Myers Squibb (BMS) patent for this study.

4.1.2. Preparation of Dasatinib Solvate Forms. 4.1.2.1. Dasatinib Hexanoic Acid (DAS-HA, 1:3) Solvate. Hexanoic acid (0.6 L) was charged into a clean and dry glass reactor (5 L) and heated till 40 ± 5 °C under stirring. Dasatinib (100 g) was

https://doi.org/10.1021/acsomega.1c06753
ACS Omega 2022, 7, 7032−7044

then charged slowly at 40 °C, and the resultant suspension was stirred further for 30 min at 40 °C. The suspension spontaneously dissolved after around 30 min of stirring, and a gummy mass in the glass reactor was observed. *n*-Heptane (0.6 L) was then charged onto the above gummy mass with stirring, and the reaction mass was maintained at 25 ± 5 °C for 6−7 h. The isolated free solid mass was filtered under vacuum and washed with *n*-heptane (0.1 L). The obtained solid was dried in a vacuum tray dryer at 40 ± 5 °C for 24 h until obtaining a constant weight to obtain around 139.5 g of the titled compound.

Yield, 81.4%.

4.1.2.2. Dasatinib Heptanoic Acid (DAS-HEA, 1:3) Solvate. The same procedure described above is followed to prepare this compound.

Yield, 82.8%.

4.1.2.3. Dasatinib Octanoic Acid (DAS-OA, 1:1) Solvate. Octanoic acid (0.7 L) was charged into a clean and dry glass reactor (5 L), and the temperature of the mass was increased to 40 ± 5 °C. Dasatinib (100 g) was then charged slowly onto the above mass at 40 °C, and the resultant suspension was maintained for 60 min at 40 °C. *n*-Heptane (0.7 L) was then charged to the hazy mass obtained above and maintained at 25 ± 5 °C for 12 h. The product isolated was filtered under vacuum and washed with *n*-heptane. The solid was dried in a vacuum tray dryer at 40 ± 5 °C for 24 h until obtaining a constant weight to obtain 108.0 g of dasatinib C_8 fatty acid solvate.

Yield, 83.4%. It is to be noted that as the crystallization process involves antisolvent precipitation, dissolution of dasatinib (completely or partially) in a solvent is essential in this case and the solvent is the solvate former itself. Hence, to dissolve dasatinib, we used an excess amount of fatty acid (100 g in 600−700 mL) in DAS-HA, DAS-HEA, and DAS-OA. Further, stoichiometry is not predicted before isolation of the solvate.

4.2. Powder X-ray Diffraction (PXRD). Powder X-ray diffraction patterns were collected using a Bruker AXS D2 PHASER diffractometer equipped with an SSD 166 detector with a detector opening of 2.003° 2θ. The target material for the generation of X-rays is copper with an X-ray wavelength of 1.5406 Å. The X-ray generator settings for the generation of X-rays are 30 kV and 10 mA. The scanning range for the test samples was selected from 3 to 40° 2θ. The step size and step time were 0.02° and 0.32 s/step, respectively. The powder X-ray diffractograms were processed using DIFFRAC.EVA software (Version Number: 4.2.0.31).

4.3. Differential Scanning Calorimetry (DSC). DSC thermograms were collected on a TA Instruments (Discovery differential scanning calorimeter) with Trios software. All of the samples were sealed in a T-zero aluminum pan with an aluminum lid and heated from 25 to 350 °C with a ramp rate of 10 °C/min under a nitrogen purge flow rate of 50 mL/min. The thermograms were processed using Universal analysis software, Version 4.5A.

4.4. Thermogravimetric Analysis (TGA). TGA thermograms were collected on a Discovery TGA550, TA Instruments, with Trios software. All of the samples were loaded with a pretarred platinum 100 μL pan and analyzed under a 60 mL/min (sample purge) flow rate environment from 25 to 350 °C with a 10 °C/min heating rate. The thermograms were processed using Universal analysis software, Version 4.5A.

4.5. Fourier Transform Infrared (FT-IR) Spectroscopy. FT-IR spectra of all of the test samples were recorded using a PerkinElmer Spectrum 100 series instrument. The test samples were prepared in the KBR matrix with a 1−4% drug load. All of the transparent KBR pellets were made using a hydraulic pellet maker at 1−4 tons pressure for a dwell time of 1−2 min. The FT-IR spectrum scan range of 400−4000 cm^{-1} with a resolution of 4 cm^{-1} and an accumulation of 16 scans was used.

4.6. Nuclear Magnetic Resonance (NMR) Spectroscopy. The solution ^{1}H-NMR spectra of all of the test samples were recorded on a Bruker AVANCE 400 WB (Bruker, Germany) at 400 MHz and ambient probe temperature in a deuterated solvent, DMSO-d_6. ^{1}H NMR spectroscopic data are given as chemical shifts in ppm from −1.0 to 16 ppm, followed by multiplicity (s, singlet; d, doublet; t, triplet; q, quartet; m, multiplet), number of protons, and coupling constants.

4.7. Temperature-Cycled DAS-HA, DAS-HEA, and DAS-OA Preparation Using TGA. DAS-HA, DAS-HEA, and DAS-OA were individually heated using a thermogravimetric analyzer (Discovery TGA550 with Trios software) up to 200 °C with a 10 °C/min ramp rate, followed by cooling to 30 °C. The desolvated DAS-HA, DAS-HEA, and DAS-OA were unloaded from the thermogravimetric analyzer and subjected individually to PXRD analysis.

4.8. DSC Analysis and TGA of Desolvated DAS-HA, DAS-HEA, and DAS-OA. The above temperature-cycled DAS-HA, DAS-HEA, and DAS-OA (each ∼10 mg) were taken out from the thermogravimetric analyzer, and ∼1 to 3 mg of each sample was placed in an aluminum pan and crimped with an aluminum lid using a crimper. The temperature program for each sample analysis was from 40 to 320 °C with a 10 °C/min ramp rate. The nitrogen gas flow rate was 50 mL/min while performing the analysis. A Discovery differential scanning calorimeter, TA Instruments, with Trios software was used for DSC analysis.

The desolvated DAS-HA, DAS-HEA, and DAS-OA in Section 4.7 were again taken in a pretarred 100 μL platinum TGA pan and subjected to TGA analysis from 40 to 350 °C with a 10 °C/min ramp rate. TGA balance and furnace purge flow rates were 40 and 60 mL/min, respectively. A Discovery TGA550, TA Instruments, with Trios software was used for TGA analysis.

4.9. Hot Stage Microscopy. Hot stage microscopic study on DAS-HA, DAS-HEA, and DAS-OA was performed using a Leica polarized light microscope (Model, DM2700P) equipped with a Linkam hot stage (Model, LTS 420 with LINK software). The test samples were individually taken onto a hot stage microscopic glass slide by spreading the powder sample properly on the microscopic slide. The prepared sample slide is inserted into the Linkam hot stage accessory (LTS 420), and using 20× magnification with a 5.0 megapixel camera, the sample is illuminated and focused. The resulting video then appears on a connected computer. The sample is heated up to 300 °C with a 5 °C/min ramp rate (LINK, version No. 1.2.20.8).

4.10. High-Performance Liquid Chromatography (HPLC). HPLC analysis was performed using a Waters 2695 series HPLC instrument with Empower 3.0 software and a Kromasil 5-C18, 125 mm × 4 mm, 5 μm column. The HPLC method parameters are as follows: flow rate of 1.0 mL/min, injection volume of 5 μL, column oven temperature of 40 °C, detector wavelength of 310 nm, and run time of 27 min.

https://doi.org/10.1021/acsomega.1c06753
ACS Omega 2022, 7, 7032−7044

Mobile phase A contains pH 6.6 ± 0.1 ammonium acetate buffer, and mobile phase B contains 90:10 v/v acetonitrile/water. A gradient program is used for the elution of the dasatinib analyte.

4.11. Gas Chromatography. The gas chromatograms of the samples were collected using an Agilent Technologies headspace autosampler GC 1290 series instrument with a DB624 capillary column (length of 75 m, diameter of 0.53 mm, and film thickness of 3 μm) and an FID detector. The method parameters are as follows: detector temperature of 260 °C; injector temperature of 140 °C; column oven temperature of 80 °C; a split ratio of 1:3; carrier gas flow rate of 4 mL/min; injection volume of 1.0 μL; carrier gas type, helium; makeup gas, nitrogen; makeup gas flow rate of 30 mL/min; and a run time of 60 min.

4.12. Water Content Using Karl Fischer Titration. Water content analysis was performed using a Metrohm 901 Titrando volumetric KF titrator. Methanol solvent was used as a blank for preparation of the sample solution. Each test sample was weighed and transferred to the titration vessel (containing blank methanol) and titrated with the Karl Fischer reagent. The reagent is standardized using disodium tartrate dihydrate and used as a KF factor for relative estimation of the water content in the samples.

5. PHYSICOCHEMICAL PROPERTIES

5.1. Powder Dissolution Study. DAS-HA, DAS-HEA, DAS-OA, and DAS Form H1-7 were taken in triplicate for dissolution testing on a Lab India DS8000 with an autosampler (USP Type II, paddle). Acetate buffer (pH 4.0) containing 1% Triton X100 (Office of Generic Drugs media)[53] medium was used for dissolution. The dissolution was under sink conditions, and the method parameters used are as follows: media volume of 1000 mL, paddle speed of 60 rpm, and temperature of 37 ± 0.5 °C. The sampling time points of the measurement were at 5, 10, 15, 30, 45, and 60 min.

5.2. Process-Induced Transformation Studies. *5.2.1. Milling.* DAS-HA, DAS-HEA, and DAS-OA (each 2.0 g) were taken in a 50 mL milling jar and milled for 30 min with 500 rpm using a Retch Planetary Ball Mill PM 100 containing 6−8 metal balls.

5.2.2. Compaction. DAS-HA, DAS-HEA, and DAS-OA (each 100 mg) were compacted at 10 tons pressure using an IR hydraulic pellet maker with a dwell time of 15 min.

5.2.3. Aqueous slurry. DAS-HA, DAS-HEA, and DAS-OA (each 1000 mg) were taken in a 10.0 mL glass vial, and 5.0 mL of purified water was added. The resulting suspension was kept in a Julabo water shaker bath (200 rpm) for 24 h at 25 ± 2 °C.

5.3. High-Humidity and -Temperature Storage. Relative humidity of 90 ± 5% is achieved using a saturated solution of potassium nitrate in a sealed glass desiccator. DAS-HA, DAS-HEA, and DAS-OA (each 1.0 g) were subjected to (open exposure) the mentioned humidity for 48 h. On the other hand, evaluation of high-temperature storage was carried out by taking 1.0 g of each DAS-HA, DAS-HEA, and DAS-OA in a Petri dish and subjecting them to open exposure at 60 ± 2 °C for 48 h in an air tray dryer (ATD).

5.4. Stability Study. A duration of 3 months is considered for the DAS-HA, DAS-HEA, and DAS-OA stability study. The packing conditions comprise placing 2.0 g of the sample in a pre-nitrogen-purged LDPE bag and tying it with a cable after removing the air. The cabled polybag was placed in a black polybag containing 1.0 g of molecular sieves and tied with a cable. The above polybag was then placed in a triple-laminated aluminum bag and sealed. The pack was stored for up to 3 months at 40 ± 2 °C and 75% ± 5% RH (accelerated conditions).

■ ASSOCIATED CONTENT

Supporting Information

The Supporting Information is available free of charge at https://pubs.acs.org/doi/10.1021/acsomega.1c06753.

Figures related to DSC, TGA, FT-IR and ^{1}H NMR, spectroscopies, and hot stage microscopy images; ORTEP diagram of DAS; PXRD overlays of DAS and DAS fatty acid solvates; and tables providing the data on *n*-heptane content by GC, powder dissolution data, process-induced transformations, and preliminary stress data of DAS fatty acid solvates (PDF)

■ AUTHOR INFORMATION

Corresponding Authors

Arthanareeswari Maruthapillai − *Department of Chemistry, SRM Institute of Science and Technology, Chennai 603203, India;* orcid.org/0000-0002-1794-3967; Phone: +91-9600112945; Email: arthanareeswari@gmail.com; Fax: 044-27453903

Vijayavitthal T. Mathad − *Polymorph Screening and Development Laboratory, R&D center, MSN Laboratories (P) Ltd., Hyderabad 502307 Telangana, India;* orcid.org/0000-0003-4507-5367; Phone: +91-9100719374; Email: drvtmathad@yahoo.co.in, drvtmathad@msnlabs.com; Fax: +91-8452-304701

Authors

Venkata Narasayya Saladi − *Department of Chemistry, SRM Institute of Science and Technology, Chennai 603203, India; Polymorph Screening and Development Laboratory, R&D center, MSN Laboratories (P) Ltd., Hyderabad 502307 Telangana, India*

Bal Raju Kammari − *Polymorph Screening and Development Laboratory, R&D center, MSN Laboratories (P) Ltd., Hyderabad 502307 Telangana, India;* orcid.org/0000-0002-8144-0862

Sudarshan Mahapatra − *Solid State and Structural Chemistry Unit, Indian Institute of Science, Bangalore 560012, India*

Ramanaiah Chennuru − *Department of Chemistry, Gitam Institute of Science and Technologies, Visakhapatnam 530045 Andhra Pradesh, India*

Eswaraiah Sajja − *Polymorph Screening and Development Laboratory, R&D center, MSN Laboratories (P) Ltd., Hyderabad 502307 Telangana, India*

Srinivasan Thirumalai Rajan − *Polymorph Screening and Development Laboratory, R&D center, MSN Laboratories (P) Ltd., Hyderabad 502307 Telangana, India*

Complete contact information is available at: https://pubs.acs.org/10.1021/acsomega.1c06753

Notes

The authors declare no competing financial interest.

■ ACKNOWLEDGMENTS

The authors thank the management of MSN Laboratories Private Limited for encouraging and supporting this work. Co-operation from project colleagues is also highly appreciated.

VNS is thankful to the department of chemistry, SRM University, for supporting this work.

REFERENCES

(1) Shariare, M. H.; Altamimi, M. A.; Marzan, A. L.; Tabassum, R.; Jahan, B.; Reza, H. M.; Rahman, M.; Ahsan, G. U.; Kazi, M. In Vitro Dissolution and Bioavailability Study of Furosemide Nanosuspension Prepared Using Design of Experiment (DoE). *Saudi Pharm. J.* **2019**, *27*, 96−105.
(2) Thayer, A. M. Finding Solutions. *Chem. Eng. News* **2010**, *88*, 13−18.
(3) https://www.gmp-compliance.org/files/guidemgr/UCM070246.pdf (accessed January 24, 2022).
(4) Shah, V. P.; Amidon, G. L. G.L. Amidon, H. Lennernas, V.P. Shah, and J.R. Crison. A Theoretical Basis for a Biopharmaceutic Drug Classification: The Correlation of In Vitro Drug Product Dissolution and In Vivo Bioavailability, Pharm Res 12, 413−420, 1995—Backstory of BCS. *AAPS J.* **2014**, *16*, 894−898.
(5) Yu, L. X.; Amidon, G. L.; Polli, J. E.; et al. Biopharmaceutics Classification System: The Scientific Basis for Biowaver Extensions. *Pharm. Res.* **2002**, *19*, 921−925.
(6) Ajay, S.; Shivani, G.; Pradip Kumar, M.; Jagabandhu, S.; Deepak, Ch. Improving solubility and intrinsic dissolution rate of ofloxacin API through salt formation via mechanochemical synthesis with diphenic acid. *J. Mol. Struct.* **2020**, *1225*, No. 128806.
(7) Serajuddin, A. T. M. Salt Formation to Improve Drug Solubility. *Adv. Drug Delivery Rev.* **2007**, *59*, 603−616.
(8) Haleblian, J. K. Characterization of Habits and Crystalline Modification of Solids and Their Pharmaceutical Applications. *J. Pharm. Sci.* **1975**, *64*, 1269−1288.
(9) Saladi, V. N.; Kammari, B. R.; Mandad, P. R.; Krishna, G. R.; Sajja, E.; Thirumalai, R. S.; Marutapillai, A.; Mathad, V. T. Novel Pharmaceutical Cocrystal of Apalutamide, a Nonsteroidal Antiandrogen Drug: Synthesis, Crystal Structure, Dissolution, Stress, and Excipient Compatibility. *Cryst. Growth Des.* **2022**, *22*, 1130−1142.
(10) Narasayya, S. V.; Maruthapillai, A.; Mahapatra, S. Discovery of a novel and pharmaceutically viable propylene glycol solvate of Idelalisib. *Mater. Today: Proc.* **2021**, *34*, 510−515.
(11) Laitinen, R.; Korbinian, L.; Holger, G.; Petra, P.; Clare, J. S.; Thomas, R. Supersaturating drug delivery systems: The potential of co-amorphous drug formulations. *Int. J. Pharm.* **2017**, *532*, 1−12.
(12) Kaushal, A. M.; Gupta, P.; Bansal, A. K. Amorphous Drug Delivery Systems: Molecular Aspects, Design, and Performance. *Crit. Rev. Ther. Drug Carrier Syst.* **2004**, *21*, 133−193.
(13) Babu, N. J.; Nangia, A. Solubility Advantage of Amorphous Drugs and Pharmaceutical Cocrystals. *Cryst. Growth Des.* **2011**, *11*, 2662−2679.
(14) Haleblian, J.; McCrone, W. Pharmaceutical Applications of Polymorphism. *J. Pharm. Sci.* **1969**, *58*, 911−929.
(15) Shi, X.; Song, S.; Ding, Z.; Fan, B.; Tu, X.; Wan, H. Improving the Solubility and Dissolution of Ibrutinib by preparing Solvates. *J. Pharm. Innovation* **2019**, *15*, 569−580.
(16) Narasayya, S. V.; Maruthapillai, A.; Sundaramurthy, D.; Selvi, J. A.; Mahapatra, S. Preparation, Pharmaceutical Properties and Stability of Lesinurad Co-crystals and Solvates. *Mater. Today: Proc.* **2019**, *14*, 532−544.
(17) Chen, J.; Sarma, B.; Evans, J. M. B.; Allan, S. M. Pharmaceutical Crystallization. *Cryst. Growth Des.* **2011**, *11*, 887−895.
(18) Xiong, X.; Qiaohong, D.; Xia, Z.; Jiawei, H.; Hongqin, Y.; Hui, L. Solvates and Polymorphs of Rebamipide: Preparation, Characterization, and Physicochemical Analysis. *RSC Adv.* **2017**, *7*, 23279−23286.
(19) Newman, A. Specialized Solid Form Screening Techniques. *Org. Process Res. Dev.* **2013**, *17*, 457−471.
(20) https://www.ema.europa.eu/en/documents/scientific-discussion/sprycel-epar-scientific-discussion_en.pdf (accessed January 24, 2022).
(21) Dasatinib pKa, log P andstructural properties are calculated using Marvin 5.10.1, ChemAxon. 2012, https://chemicalize.com/#/calculation.
(22) Lajeunesse, J.; DiMarco, D.; Galella, M.; Chidambaram, R. Processfor Prepararing 2-Aminothiazole-5-Aromatic Carboxamides as Kinase Inhibitors. US7,491,725B22009.
(23) Simo, O.; Filipcick, J.; Martaus, A.; Jegorov, A.; Gavenda, A.; Aronhime, J.; Vraspir, P.; Koltai, T.; Faustmann, J.; Gabriel, R. Polymorphs of Dasatinib Isopropyl Alcohol and Process for Preparation Thereof. US8,067,423B22011.
(24) Vraspir, P.; Gavenda, A.; Gabriel, R.; Jegorov, A. Polymorphs of Dasatinib and Process for Preparation Thereof. WO2010/062715 A22010.
(25) Sarceviča, I.; Grante, I.; Belyakov, S.; Rekis, T.; Bērziņš, K.; Actiņš, A.; Orola, L. Solvates of Dasatinib: Diversity and Isostructurality. *J. Pharm. Sci.* **2016**, *105*, 1489−1495.
(26) Ahmadi, S.; Mondal, P. K.; Mirmehrabi, M.; Rohani, S. Desolvation of Dasatinib Methanolate: An Improved Anhydrous Polymorph. *CrystEngComm* **2021**, *23*, 4272−4283.
(27) Roy, S.; Rosalynn, Q.; Matzger, A. J. Structural and Physicochemical Aspects of Dasatinib Hydrate and Anhydrate Phases. *Cryst. Growth Des.* **2012**, *12*, 2122−2126.
(28) Grant, D. J. W.; Abougela, I. K. A. Fatty Acid Solvates of Griseofulvin. *J. Pharm. Pharmacol.* **1979**, *31*, No. 49P.
(29) Shanmukha Prasad, G.; Venkata Narasayya, S.; Peddy, Vishweshwar.; Rajeev Budhdev, R. Solid Forms of Ibrutininb. WI2019/138326WO2019.
(30) Stability testing of new drug substances and products. International Conference on Harmonization (ICH) Q1A. https://www.ich.org/fileadmin/PublicWeb_Site/ICH_Products/Guidelines/Quality/Q1A_R2/Step4/Q1A_R2Guideline.pdf (accessed January 18, 2018).
(31) Eckert, F.; Klamt, A. Fast Solvent Screening via Quantum Chemistry: COSMO-RS Approach. *AIChE J.* **2002**, *48*, 369−385.
(32) Eckert, F.; Klamt, A.. *KG, Leverkusen, Ger*, COSMOtherm, version C2. 1, Release 01.05, COSMOlogic GmbH & Co., 2006.
(33) Klamt, A. The COSMO and COSMO-RS solvation models. *Wiley Interdiscip. Rev.: Comput. Mol. Sci.* **2011**, *1*, 699−709.
(34) Marsh, K. N. COSMO-RS: From Quantum Chemistry to Fluid PhaseThermodynamics and Drug Design By A. Klamt. Elsevier: Amsterdam, The Netherlands, 2005. 246 pp. $US 165. ISBN 0-444-51994-7. *J. Chem. Eng. Data* **2006**, *51*, 1480.
(35) Lemmerer, A.; Stefan, G.; Marcelle, J.; Xolani, M.; Kelsey, L. S. Co-crystals and molecular salts of carboxylic acid/pyridine complexes: Can calculated pKa's predict proton transfer? A case study of nine complexes. *Cryst. Eng. Comm.* **2015**, *17*, 3591−3595.
(36) Childs, S. L.; Staly, G. P.; Park, A. The salt-cocrystal continuum: The influence of crystal structure on ionization state. *Mol. Pharm.* **2007**, *4*, 323−338.
(37) Aitipamula, S.; Banerjee, R.; Bansal, A. K.; Biradha, K.; Cheney, M. L.; Choudhury, A. R.; Desiraju, G. R.; Dikundwar, A. G.; Dubey, R.; Duggirala, N.; Ghogale, P. P.; Ghosh, S.; Goswami, P. K.; Goud, N. R.; Jetti, R. R. K. R.; Karpinski, P.; Kaushik, P.; Kumar, D.; Kumar, V.; Moulton, B.; Mukherjee, A.; Mukherjee, G.; Myerson, A. S.; Puri, V.; Ramanan, A.; Rajamannar, T.; Reddy, C. M.; Rodriguez-Hornedo, N.; Rogers, R. D.; Guru Row, T. N.; Sanphui, P.; Shan, N.; Shete, G.; Singh, A.; Sun, C. C.; Swift, J. A.; Thaimattam, R.; Thakur, T. S.; Thaper, R. K.; Thomas, S. P.; Tothadi, S.; Vangala, V. R.; Variankaval, N.; Vishweshwar, P.; Weyna, D. R.; Zaworotko, M. J. Polymorphs, Salts and Cocrystals: Whats in a Name? Cryst. *Growth Des.* **2012**, *12*, 2147−2152.
(38) Stahly, G. P. Diversity in Single-and Multiple-Component Crystals. The Search for and Prevalence of Polymorphs and Cocrystals. *Cryst. Growth Des.* **2007**, *7*, 1007−1026.
(39) Boultif, A.; Louër, D. Indexing of Powder Diffraction Patterns for Low-Symmetry Lattices by the Successive Dichotomy Method. *J. Appl. Crystallogr.* **1991**, *24*, 987−993.

https://doi.org/10.1021/acsomega.1c06753
ACS Omega 2022, 7, 7032−7044

(40) Neumann, M. A. X-Cell: A Novel Indexing Algorithm for Routine Tasks and Difficult Cases. *J. Appl. Crystallogr.* **2003**, *36*, 356−365.
(41) Pawley, G. S. Unit-Cell Refinement from Powder Diffraction Scans. *J. Appl. Crystallogr.* **1981**, *14*, 357−361.
(42) Kohsaku, K.; Vyazovkin, S.; Koga, N.; Schick, C. *Handbook of Thermal Analysis and Calorimetry*; Elsevier Science B.V., 2018; Chapter 15, Vol. *6*, pp 613−641.
(43) Giron, D. Aplications of Thermal Analysis and Coupled Techniques in Pharmaceutical Industry. *J. Therm. Anal. Calorim.* **2002**, *68*, 335−357.
(44) Garbacz, P.; Wesolowski, M. FTIR and Raman Spectroscopy Coupled with Multivariate Analysis in a Study of Co-Crystals of Pharmaceutical Interest. *Molecule* **2018**, *23*, No. 2136.
(45) Hameed, I. H.; Al-Rubaye, A. F.; Kadhim, M. J. Uses of Nuclear Magnetic Resonance Spectroscopy Technique in Pharmaceutical Analysis: A Review. *Int. J. Curr. Pharm. Rev. Res.* **2017**, *8*, 79−84.
(46) Chadha, R.; Astha, K.; Punam, A.; Kishor, S. Characterisation and Evaluation of Pharmaceutical Solvates of Atorvastatin Calcium by Thermoanalytical and Spectroscopic Studies. *Chem. Cent. J.* **2012**, *6*, No. 114.
(47) Kumar, A.; Pritam, S.; Arun, N. Hot Stage Microscopy and Its Applications in Pharmaceutical Characterization. *Appl. Microsc.* **2020**, *50*, No. 12.
(48) Suarez-Sharp, S.; Michael, C.; Filippos, K.; Andreas, A.; Patrick, M.; Poonam, D.; Evangelos, K.; Min, L.; Anna, N.; Nagesh, B.; et al. Applications of Clinically Relevant Dissolution Testing: Workshop Summary Report. *AAPS J.* **2018**, *20*, No. 93.
(49) Anand, O.; Yu, L. X.; Conner, D. P.; Davit, B. M. Dissolution Testing for Generic Drugs: An FDA Perspective. *AAPS J.* **2011**, *13*, No. 328.
(50) Schneider-Rauber, G.; Arhangelskis, M.; Bond, A. D.; Ho, R.; Nere, N.; Bordawekar, S.; Sheikh, A. Y.; Jones, W. Polymorphism and Surface Diversity Arising From Stress-Induced Transformations − The Case of Multicomponent Forms of Carbamazepine. *Acta Crystallogr., Sect. B: Struct. Sci., Cryst. Eng. Mater.* **2021**, *77*, 54−67.
(51) Zhang, G. Z.; Law, D.; Schmitt, E. A.; Qiu, Y. Phase Transformation Considerations during Process Development and Manufacture of Solid Oral Dosage Forms. *Adv. Drug Delivery Rev.* **2004**, *56*, 371−390.
(52) https://www.cfsanappsexternal.fda.gov/scripts/fdcc/?set=SCOGS&sort=Sortsubstance&order=ASC&startrow=1&type=basic&search=Caprylic%20acid (accessed September 6, 2021).
(53) https://www.accessdata.fda.gov/scripts/cder/dissolution/dsp_SearchResults.cfm (accessed January 24, 2022).

https://doi.org/10.1021/acsomega.1c06753
ACS Omega 2022, 7, 7032−7044